Histological examination of choroid plexus epithelia changes in schizophrenia.

Williams MR[1], Macdonald[2] CM & Turkheimer F[3]

1. Segmentum Analysis, Innovation Building, Biocity, Nottingham, UK. 2. Clerkenwell Health, Aldersgate Street, London, UK. 3. Institute of Psychiatry, King's College London, UK

Abstract

Background: The choroid plexus (CP) is suggested to be involved in neuroimmune regulation avia the interaction between central and peripheral inflammation. Quantitative imaging has demonstrated volumetric CP change in psychosis, schizophrenia and depression. This study histologically examines CP epithelial cell morphology in these illnesses to identify the biological source of such volumetric changes.

Methods: Formalin-fixed paraffin-embedded FFPE blocks were obtained bilaterally from the lateral ventricles of 13 cases of sex- and age-matched brains from each of schizophrenia (SZ) with psychosis, major depressive disorder (MDD) and matched controls. FFPE blocks were sectioned at 7μm and routinely stained for H&E. Morphological analysis of 180 CP epithelia/case was conducted blindly on digital images collected x600 magnification. Calcification was assessed in all CP regions manually.

Results: Linear General Model analysis shows a significant effect of diagnosis on somal width ($p=0.006$, $r^2=0.33$, adj=0.25), with a significant difference between SZ non-medicated v non-medicated NPD controls ($p=0.032$), demonstrating increased somal width in SZ with psychotic medication but not in unmedicated SZ cases. No effects were observed in calcification.

Discussion: Epithelial cells examined were adhered to CP fibrous surface so width expansion describes the primary methods for these cells to expand with adherence to this surface. The interaction of antipsychotic medication and diagnosis demonstrates that this is an illness-specific change and mediated through the DA-system, although the mechanism is unclear at present.

Keywords

Schizophrenia, Major depressive Disorder, Pathology, Choroid Plexus, Dopamine

Introduction

The choroid plexus (CP) has been identified as a distinct structure for many years and investigated for its possible role in the pathophysiology of schizophrenia (SZ) for over a century[1-3]. The CP is important for the secretion of cerebrospinal fluid (CSF). It is formed of a vascularized stroma with loose connective tissue with a single outer layer of epithelia continuous with the ependyma lining the brain of lateral, 3rd and 4th ventricles, as well as often found on the outer surface of the brain[4-6]. The CP is suggested to be regulated by descending neurons and by circulating factors. High receptor concentrations for circulating hormones and serotonin, atrial natriuretic peptide, vasopressin and the insulin-like growth factors have been reported in the CP and shown to affect its function[7].

The CNS is protected against substances from the blood by the blood–brain barrier (BBB) and the blood–cerebrospinal barrier[8-11]. CP epithelial cells form the blood–cerebrospinal fluid barrier, controlling CSF secretion into the ventricular system[12]. The production of CSF from blood plasma in the CP is performed by a filtration process to remove unneeded plasma proteins, controlling CSF protein content[8,13]. The blood–cerebrospinal barrier has a key role in the spreading of inflammatory reactions from the peripheral regions to the CNS and has been suggested to contribute to the pathogenesis and progression of various neurological disorders[14-16], demonstrated by the report that up to 40% of patients with inflammatory bowel disease present with psychosocial disturbances[17].

Recently, CP imaging abnormalities have been reported in psychiatric cohorts. In patients with SZ, CP volume has been found consistently larger compared to controls[18-20], whereas the enlargement has demonstrated a genetic component as it was intermediate in first-degree relatives[18]. This finding has been repeated trans-diagnostically as greater CP volume has also been demonstrated in patients with Major Depression Disorder (MDD)[20]. There is evidence of CP enlargement with measures of inflammation, either peripheral or central, and stress. In patients with SZ - a positive association has been demonstrated with peripheral plasma IL-6 levels and allostatic load[18,19]. In MDD, CP volume has been associated with neuroinflammation measured with positron emission tomography (PET) in the anterior cingulate cortex, prefrontal cortex and insular cortex, but not with peripheral inflammatory markers[20]. Notably CP enlargement has been recently proposed as a transdiagnostic marker of brain inflammation in neurodegenerative conditions[21].

Imaging studies in-vivo are limited though as they may not generally indicated the cellular bases of CP volumetric changes. A small CT-MRI study of 12 SZ patients under 45y has implicated calcification in the CP volumetric changes following neuroleptic treatment[22,23]. Calcification of the CP as measured by quantitative imaging has been implicated in serotonin function in SZ and as a marker of depression[24,25].

The aim of this neuropathological study was to verify the cellular abnormalities associated with CP volumetric changes in SZ and MDD cohorts. Specifically, we apply digital histopathological methods to examine the morphology of epithelial cells in CP from the lateral ventricles, and manual examination of CP calcification from multiple brain areas from human neuropathological samples from control, SZ with psychosis and MDD cases.

Methods

Cases

Cases were sourced from the Corsellis brain collection, selected for age of death between 45-60 and re-reviewed for inclusion by modern criteria as defined by ICD-10 by a senior consultant psychiatrist. SZ cases all contained first-rank symptoms with onset below 30 years, with positive symptomatology including psychosis with auditory hallucinations. MDD cases were included with repeated cycles of treatment-resistant depression with onset under 25 years. Cases were included only if they had substantial tissue available for use with full clinical and psychiatric files with drug histories and passed neuropathological review to exclude confounding pathology. A breakdown of cases included in this study is shown in Table 1.

Case	Age/y	Sex	Diagnosis	PM/h	Fix/y	Suicide	Cause of death
1	51-55	M	NPD	82	38	N	Heart Failure from COPD
2	45-50	F	NPD	23	30	N	Non-follicular lymphoma
3	45-50	M	NPD	61	39	N	Lymphoid leukaemia
4	56-60	F	NPD	98	26	N	Chronic ischaemic heart disease
5	51-55	M	NPD	24	29	N	Congestive heart failure
6	51-55	F	NPD	36	35	N	Malignant neoplasm of stomach
7	56-60	F	NPD	NK	40	N	Pneumonia
8	51-55	F	NPD	54	45	N	Acute myocardial infarction
9	56-60	F	NPD	60	40	N	Pneumonia
10	51-55	M	NPD	56	39	N	Acute myocardial infarction
11	45-50	M	NPD	32	37	N	Acute myocardial infarction
12	56-60	M	NPD	55	40	N	Atherosclerosis
13	51-55	F	NPD	24	41	N	Gastrointestinal haemorrhage
14	56-60	F	SZ	NK	51	N	Pneumonia
15	45-50	M	SZ	46	26	Y	Suicide
16	56-60	F	SZ	22	39	N	Pulmonary embolism
17	56-60	M	SZ	28	38	N	Congestive heart failure
18	51-55	F	SZ	28	46	N	Pulmonary embolism
19	56-60	M	SZ	58	47	N	Post-operative complications
20	56-60	M	SZ	24	41	N	Acute myocardial infarction
21	56-60	F	SZ	26	38	N	Congestive heart failure
22	45-50	M	SZ	91	47	N	Congestive heart failure
23	45-50	M	SZ	29	47	N	Acute myocardial infarction
24	56-60	F	SZ	19	40	Y	Intentional self-harm by hanging
25	56-60	F	SZ	26	42	N	Acute myocardial infarction
26	56-60	F	SZ	41	48	N	Kidney Failure
27	45-50	F	MDD	66	30	Y	Intentional self-poisoning
28	51-55	F	MDD	63	27	Y	Intentional self-poisoning

29	45-50	M	MDD	26	24	N	Asphyxiation
30	51-55	F	MDD	22	28	Y	Suicide
31	56-60	M	MDD	NK	31	N	Pulmonary embolism
32	45-50	M	MDD	17	30	Y	Intentional CO poisoning
33	45-50	F	MDD	28	31	Y	Intentional self-poisoning
34	45-50	M	MDD	16	25	Y	Intentional CO poisoning
35	56-60	M	MDD	NK	33	Y	Intentional self-harm by jumping
36	51-55	M	MDD	73	35	Y	Intentional self-harm by jumping
37	56-60	F	MDD	NK	33	N	Pneumonia
38	56-60	F	MDD	52	35	N	Acute myocardial infarction
39	56-60	M	MDD	21	38	N	Pneumonia

Table 1. NPD- no psychiatric disorder, SZ- schizophrenia, MDD- major depressive disorder, NK- not known.

Tissue source and processing

The tissue was originally from the Corsellis brain collection, formerly the Runwell collection[26], currently held at the Gordon Pathology Museum (Guys Campus, KCL, London, UK). Dissection was conducted in the museum processing rooms consistent with previous neuropathology projects[27-32]. CP tissue was dissected bilaterally from the lateral ventricles of cases described in Table 1. Right and left lateral ventricles were found within coronal sections and removed separately for each ventricle, stored in a single pathology cassette for each case, with dissection markers to distinguish laterality. Bilateral CP samples were obtained from all cases. Dissected tissue was contained in standard pathology cassettes and transported in 10% formalin (4% v/v).

Tissue processing, sectioning and staining was conducted by Histologix Ltd (Nottingham, UK) using routine methods and embedded into paraffin blocks. Formlin-Fixed Paraffin-Embedded (FFPE) blocks were sectioned by microtome at 7μm and mounted on electrostatic 75x25mm slides. Routine H&E staining was performed on all sections with Harris Hematoxylin and 50/50 aqueous Eosin using a Leica ST4040 linear slide stainer (Leica, Germany).

Image collection

Images were collected on a single Olympus Microtec microscope (Tokyo, Japan) at x600 total magnification using a 10MP USB 2.0 Colour CMOS C-Mount Microscope Camera (Amscope, USA) at 3584x2748 resolution.

Initially CP tissue was identified at x150 magnification. For each image a grid mask was imposed and a random number generator (www.calculator.net) used to select sampling regions to remove selection bias.

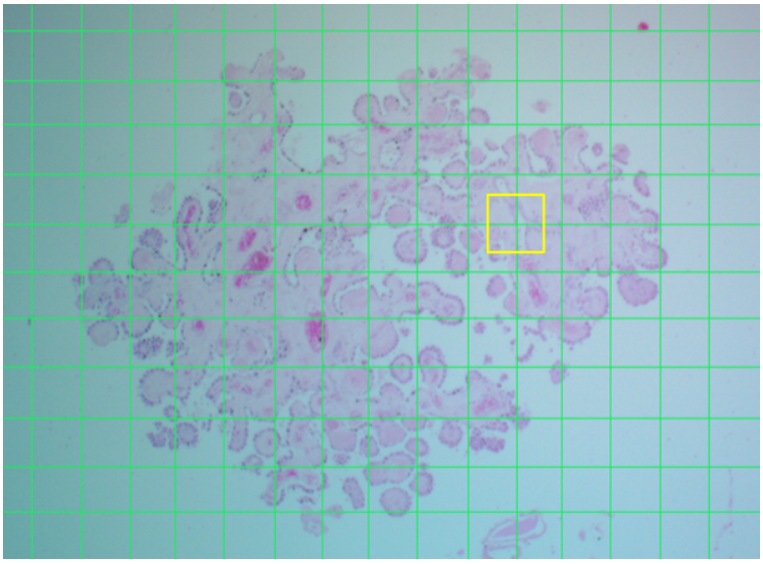

Fig. 1. H&E-stained CP at x150 magnification with grid mask (Green). Yellow square indicates region taken at x600 magnification for measurement.

Regions containing >30 measurable epithelia, as defined by inclusion criteria, were taken from each hemisphere per slide to give 2 regions sampled per slide. This was conducted on 3 slides per case to give a total of 6 regions containing 180 measured cells per case.

Experimental measures were made using a rubber stylus and touchscreen interface on an IPad Air2 device using the Segmentum Imaging v1.1 App (Segmentum Analysis Ltd, UK). This was done through serial measurement of graticule-calibrated whole image analysis using ruler and region functions for measurement of distances and circumferences/areas respectively. Data was collected blind to case identification.

Assays and measurements

Epithelial cells for measurement were identified from images captured as described. CP cells for measures were defined as “surface-based epithelial cells attached to the basal substrate with clear membranes and visible nucleus”, shown in Fig 2.

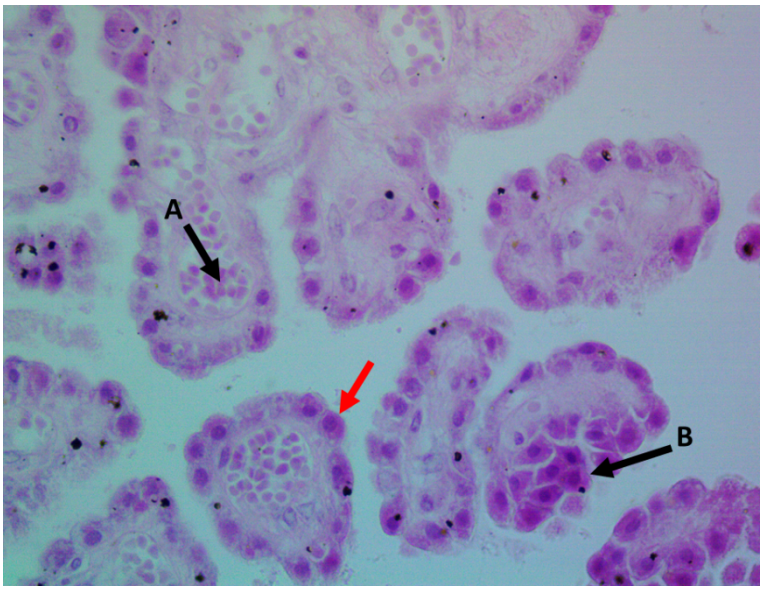

Fig. 2. H&E-stained CP at x600 magnification. Red arrow indicates epithelial cell for measurement. A – erythrocytes in blood vessel, B – epithelial cell not included for measurement due to not being attached to the basal substrate.

Repeated measures assays were conducted on 67 CP epithelia encompassing two randomly selected cases to determine statistically significant *n* size. Measures tested were:

1. Cell length - defined as the longest distance between the basal surface and the opposing cell membrane.
2. Cell width - defined as the longest distance between cell membrane surfaces not connected to the basal surface.
3. Cell circumference - defined as the length of the continuous outer membrane.
4. Cell cross sectional area - defined as the measured area of the cell bound by its outer membrane.
5. Nucleus length - defined as the distance of the cell nucleus at its longest axis.
6. Nucleus width - defined as the widest point of the nucleus perpendicular to the nucleus length.
7. Nucleus circumference - defined as the length of the outer surface of the nucleus.
8. Nuclear cross-sectional area - defined as the measured area of the nucleus bound by its outer membrane.

Somal measures on an example epithelial cell are described in Fig. 3. Nuclear measures were conducted in a similar fashion.

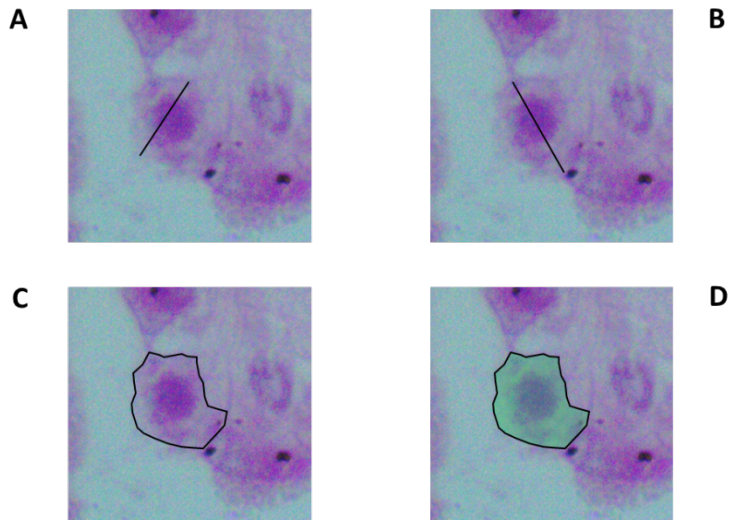

Fig. 3. H&E-stained CP at x600 magnification. Red arrow indicates epithelial cell for measurement. A – Somal length, B – Somal width, C - Somal circumference, D – Somal cross sectional area.

Repeated measures demonstrated that the appropriate minimum sample size was 30 cells measured per image to meet the required *n* size for all scalar measures (Table 2).

Measure	Ideal n size
Cell length	30
Cell width	25
Cell circumference	25
Cell CSA	NA
Nucleus length	20
Nucleus width	20
Nucleus circumference	30
Nucleus CSA	NA

Table 2. Ideal n sizes for each of the measures. NA – Not Applicable.

Experimentally each case involved measurement of 30 cells per image, 3 images per hemisphere, bilateral measures giving 6 images per slide. This resulted in the measurement of 180 cells per case by methods consistent with previous pathology studies[28,29,32].
Intra-rator errors were <5% for all measures.

Calcification

Calcification of CP in various ventricular regions was assessed semi-quantitatively. The areas of CP analysed were right and left lateral ventricles, 3rd ventricle, cerebral aqueduct, surrounding surfaces of the brainstem and pons and the outer surface of the frontal lobe.

CP was not found in one region of each of 4 cases (11/91, 107/86, 48/88, 31/90). These were not the same regions absent in any case. Tissue was manually assessed whilst in formalin, with CP in each area manually rated as having no calcification, a small amount of calcification, a significant amount of calcification or was completely calcified.

Statistical analysis

Measures were first tested using a general linear model (GLM) where independent factors were diagnostic group, age and antipsychotic use. Given the number (eight) of different measures used multiple testing correction was considered and performed via the Bonferroni correction. Only for those measures where the GLM was significant ($p<0.05$ corrected), post-hoc F tests were then performed based on linearly independent pairwise comparisons among the estimated marginal means.
Statistical analysis was run using SPSS v28.0.0.1 (IBM Corp).

Ethics

This project was conducted under ethical permission from Brain UK review number 003/12.

Results

Linear General Model analysis showed a significant effect of diagnosis on somal width (p=0.006, r^2=0.33, adj=0.25) that survived Bonferroni correction. There was a significant difference between SZ non-medicated v non-medicated NPD controls (p=0.032m Fig. 4), demonstrating increased somal width in SZ with psychotic medication but not in unmedicated SZ cases. Age was also positively associated with somal width (p=0.048).

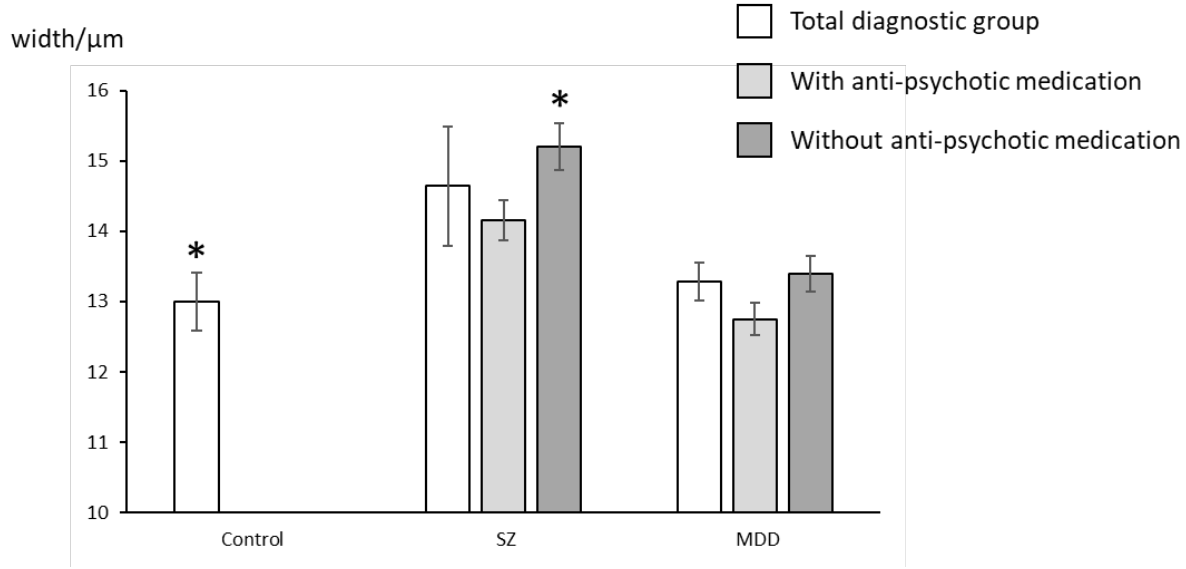

Fig. 4. Somal width by diagnosis and anti-psychotic treatment. *represents significant difference between controls and SZ without medication (LGM, p=0.032). Data shown as mean ± SEM.

No significant associations with independent factors were observed in somal length, circumference or cross-sectional area, and no changes were observed in nuclear morphology, and no effects were observed in calcification (data shown in Tables 3 & 4).

	S. Length	S. Width	S. Circ.	S. CSA	N. length	N. width	N. Circ.	N. CSA
Controls	13.8 (0.29)	13.0 (0.42)	39.7 (0.90)	108 (5.3)	6.94 (0.25)	5.13 (0.20)	17.8 (0.29)	24.1 (1.6)
SZ	14.0 (0.29)	14.6 (0.84)	42.7 (3.0)	111 (4.5)	7.22 (0.18)	5.48 (0.15)	18.2 (0.25)	23.7 (0.63)
MDD	14.3 (0.23)	13.3 (0.27)	40.3 (0.68)	121 (11)	7.17 (0.11)	5.32 (0.13)	18.5 (0.25)	24.3 (0.84)

Table 3. Means of measures for diagnostic groups. S – Somal, N – Nuclear, CSA - Cross Sectional Area. Data shown as µm, except for CSA results shown as µm². Data shown as mean (3sf) ± SEM to (2sf).

	RLV	LLV	3rd V.	4th V.	Cer. Out.	Ctx. Out.
Controls	0.31 (0.13)	0.45 (0.18)	0.69 (0.26)	0.38 (0.18)	0.15 (0.10)	0.53 (0.22)
SZ	0.31 (0.17)	0.38 (0.18)	0.77 (0.32)	0.38 (0.21)	0.15 (0.10)	0.53 (0.22)
MDD	0.31 (0.13)	0.54 (0.24)	0.70 (0.29)	0.50 (0.19)	0.30 (0.17)	0.30 (0.21)

Table 4. Calcification results by diagnostic group. RLV – Right Lateral Ventricles, LLV – Left Lateral Ventricle, 3rd V – Third Ventricle, 4th V – Fourth Ventricle, Cer Out – Outer surface around cerebellum, Ctx Out – Outer surface of frontal lobe cortex. NB: 4th ventricle describes the area around the upper part of the brainstem distinct from the cerebellum also. Data shown as mean ± SEM to 2sf.

Discussion

The main finding of this work is a significant increase in the somal width of epithelial cells in the CP of SZ cases. The epithelial cells examined were adhered to the CP fibrous surface, therefore width expansion is the primary method for expansion a cell to expands and has multiple possible causes. It could originate from changes between the cells and the blood capillaries, changes in the gap and tight junctions between the cells themselves, from the altering of their structural organisation, or from within the cells themselves. The cause of such changes could be from descending neural projections, endocrine routes or perhaps from other peripheral sources.

The interaction of antipsychotic medication and diagnosis demonstrates that this is an illness-specific change and mediated through the DA-system, although the mechanism is unclear at present. Rat CP contains DA receptor proteins, with D1 receptors predominantly expressed in the epithelium and the arterial smooth muscles and D2 receptors expressed in sympathetic fibres innerving CP epithelium and vasculature[33]. DA infusion has been demonstrated to increase blood flow through the CP in the brain of the sheep[34], and in mice DA genetic-hypofunction reduces CP permeability[35]. This finding adds to previous evidence in pre-clinical models on dopaminergic modulation of CP functionality as a promising therapeutic strategy for neurodevelopmental and psychiatric disorders.

Although we were able to demonstrate CP volumetric alterations in the brains of subjects with SZ, we did not find such alterations in MDD patients, although increased CP volume has been demonstrated by imaging in an MDD cohort that largely presented with heightened peripheral immunity and such state may not be represented in the cohort used here for which allostatic load was not available[22].

Methodologically, measurement of epithelial CP has several difficulties to overcome due to the nature of the tissue. The cell organisation is likely the reason behind the very high number of cells that had to be measured by case to get useful results. Nucleoli measures could not be conducted due to the rare visibility of nucleoli in the epithelia present, with it being unusual to even see one clear nucleolus in 30 nuclear assessments in an image.

If further assays could be developed it may be possible to quantitatively assess the calcification in these samples microscopically, although given the null macroscopic result presented and the rare occurrence on the slides this would be of questionable value.

Further pathological examination of CP tissue for GFAP or S100β as astrocyte markers may yield insights in to CP disruption, as astrocytes are known to be affected across wide regions of the brain in SZ[28,30,36-41], and have a particular role in inflammation[42,43], having a role in CP structure and function as in the CNS[44,45].

Evans blue stain has been successfully used to examine BBB integrity in live rodents[46,47], and has been successfully used to identify regions of BBB damage by injection of an Evans Blue-Hoechst cocktail for pathological analysis[48]. It is still used *in vivo* for medical diagnostics[49]. Evans Blue has also been demonstrated to be a marker of cell death or damage in plants[50-52]. Although plant cells are notably different from animal cells, the Evans Blue stain identifies such damage by membrane permeability, which may have value in translation to animal pathology.

Acknowledgements

This project was funded by the funded by the NIHR Maudsley Biomedical Research Centre at South London and Maudsley NHS Foundation Trust and King's College London.
Tissue samples were obtained from Guy's and St Thomas' NHS Foundation Trust as part of BRAIN UK, supported by Brain Tumour Research, the British Neuropathological Society and the Medical Research Council, Ethics ref: Brain UK 12/003 - Neuropathological examination of neurons, glial cells, axons and molecular factors in mood and affective disorders[53].
The authors would like to acknowledge the support of the Mr. William Edwards Gordon Pathology Museum at Kings College London Bridge campus for his care of the tissue and support of dissection, storage and transport.
Dr. Williams is inventor of Segmentum Imaging, the pathology software used in this study, and director of the Segmentum Analysis. This software was provided free for this study.

References

1. Kitabayashi S. The choroid plexuses in organic disease of the brain and in schizophrenia. The Journal of Nervous and Mental Disease1922. p. 21-26.
2. Mortazavi MM, Griessenauer CJ, Adeeb N, et al. The choroid plexus: a comprehensive review of its history, anatomy, function, histology, embryology, and surgical considerations. *Childs Nerv Syst*. Feb 2014;30(2):205-14. doi:10.1007/s00381-013-2326-y
3. Zappaterra MW, Lehtinen MK. The cerebrospinal fluid: regulator of neurogenesis, behavior, and beyond. *Cell Mol Life Sci*. Sep 2012;69(17):2863-78. doi:10.1007/s00018-012-0957-x
4. Prasongchean W, Vernay B, Asgarian Z, Jannatul N, Ferretti P. The neural milieu of the developing choroid plexus: neural stem cells, neurons and innervation. *Front Neurosci*. 2015;9:103. doi:10.3389/fnins.2015.00103
5. Lehtinen MK, Bjornsson CS, Dymecki SM, Gilbertson RJ, Holtzman DM, Monuki ES. The choroid plexus and cerebrospinal fluid: emerging roles in development, disease, and therapy. *J Neurosci*. Nov 6 2013;33(45):17553-9. doi:10.1523/jneurosci.3258-13.2013
6. Liddelow SA, Dziegielewska KM, Ek CJ, et al. Mechanisms that determine the internal environment of the developing brain: a transcriptomic, functional and ultrastructural approach. *PLoS One*. 2013;8(7):e65629. doi:10.1371/journal.pone.0065629
7. Nilsson C, Lindvall-Axelsson M, Owman C. Neuroendocrine regulatory mechanisms in the choroid plexus-cerebrospinal fluid system. *Brain Res Brain Res Rev*. May-Aug 1992;17(2):109-38. doi:10.1016/0165-0173(92)90011-a
8. Abbott NJ, Patabendige AA, Dolman DE, Yusof SR, Begley DJ. Structure and function of the blood-brain barrier. *Neurobiol Dis*. Jan 2010;37(1):13-25. doi:10.1016/j.nbd.2009.07.030
9. Hladky SB, Barrand MA. Mechanisms of fluid movement into, through and out of the brain: evaluation of the evidence. *Fluids Barriers CNS*. 2014;11(1):26. doi:10.1186/2045-8118-11-26
10. Johanson CE, Duncan JA, Stopa EG, Baird A. Enhanced prospects for drug delivery and brain targeting by the choroid plexus-CSF route. *Pharm Res*. Jul 2005;22(7):1011-37. doi:10.1007/s11095-005-6039-0
11. Lorenzo AV. Factors governing the composition of the cerebrospinal fluid. *Exp Eye Res*. 1977;25 Suppl:205-28. doi:10.1016/s0014-4835(77)80019-5
12. Brown PD, Davies SL, Speake T, Millar ID. Molecular mechanisms of cerebrospinal fluid production. *Neuroscience*. 2004;129(4):957-70. doi:10.1016/j.neuroscience.2004.07.003
13. Neuwelt EA, Abbott NJ, Drewes L, et al. Cerebrovascular Biology and the various neural barriers: challenges and future directions. *Neurosurgery*. Mar 1999;44(3):604-8; discussion 608-9. doi:10.1097/00006123-199903000-00095
14. Bors L, Tóth K, Tóth EZ, et al. Age-dependent changes at the blood-brain barrier. A Comparative structural and functional study in young adult and middle aged rats. *Brain Res Bull*. May 2018;139:269-277. doi:10.1016/j.brainresbull.2018.03.001
15. Parikh V, Tucci V, Galwankar S. Infections of the nervous system. *Int J Crit Illn Inj Sci*. May 2012;2(2):82-97. doi:10.4103/2229-5151.97273
16. Zhao Z, Nelson AR, Betsholtz C, Zlokovic BV. Establishment and Dysfunction of the Blood-Brain Barrier. *Cell*. Nov 19 2015;163(5):1064-1078. doi:10.1016/j.cell.2015.10.067
17. Carloni S, Bertocchi A, Mancinelli S, et al. Identification of a choroid plexus vascular barrier closing during intestinal inflammation. *Science*. Oct 22 2021;374(6566):439-448. doi:10.1126/science.abc6108
18. Lizano P, Lutz O, Ling G, et al. Association of Choroid Plexus Enlargement With Cognitive, Inflammatory, and Structural Phenotypes Across the Psychosis Spectrum. *Am J Psychiatry*. Jul 1 2019;176(7):564-572. doi:10.1176/appi.ajp.2019.18070825
19. Zhou YF, Huang JC, Zhang P, et al. Choroid Plexus Enlargement and Allostatic Load in Schizophrenia. *Schizophr Bull*. Apr 10 2020;46(3):722-731. doi:10.1093/schbul/sbz100

20. Senay O, Seethaler M, Makris N, et al. A preliminary choroid plexus volumetric study in individuals with psychosis. *Hum Brain Mapp*. Feb 6 2023;doi:10.1002/hbm.26224
21. Fleischer V, Gonzalez-Escamilla G, Ciolac D, et al. Translational value of choroid plexus imaging for tracking neuroinflammation in mice and humans. *Proc Natl Acad Sci U S A*. Sep 7 2021;118(36)doi:10.1073/pnas.2025000118
22. Althubaity N, Schubert J, Martins D, et al. Choroid plexus enlargement is associated with neuroinflammation and reduction of blood brain barrier permeability in depression. *Neuroimage Clin*. 2022;33:102926. doi:10.1016/j.nicl.2021.102926
23. Marinescu I, Udriştoiu I, Marinescu D. Choroid plexus calcification: clinical, neuroimaging and histopathological correlations in schizophrenia. *Rom J Morphol Embryol*. 2013;54(2):365-9.
24. Bersani G, Garavini A, Taddei I, Tanfani G, Pancheri P. Choroid plexus calcification as a possible clue of serotonin implication in schizophrenia. *Neurosci Lett*. Jan 15 1999;259(3):169-72. doi:10.1016/s0304-3940(98)00935-5
25. Sandyk R, Kay SR, Merriam AE. Calcification of the choroid plexus as a marker of depression in schizophrenia. *Schizophr Res*. 1990:361-3. vol. 5-6.
26. Kasper BS, Taylor DC, Janz D, et al. Neuropathology of epilepsy and psychosis: the contributions of J.A.N. Corsellis. *Brain*. Dec 2010;133(Pt 12):3795-805. doi:10.1093/brain/awq235
27. Williams MR, Harb H, Pearce RK, Hirsch SR, Maier M. Oligodendrocyte density is changed in the basolateral amygdala in schizophrenia but not depression. *Schizophr Res*. Jul 2013;147(2-3):402-3. doi:10.1016/j.schres.2013.04.013
28. Williams MR, Marsh R, Macdonald CD, et al. Neuropathological changes in the nucleus basalis in schizophrenia. *Eur Arch Psychiatry Clin Neurosci*. Sep 2013;263(6):485-95. doi:10.1007/s00406-012-0387-7
29. Williams MR, Galvin K, O'Sullivan B, et al. Neuropathological changes in the substantia nigra in schizophrenia but not depression. *Eur Arch Psychiatry Clin Neurosci*. Jun 2014;264(4):285-96. doi:10.1007/s00406-013-0479-z
30. Williams M, Pearce RK, Hirsch SR, Ansorge O, Thom M, Maier M. Fibrillary astrocytes are decreased in the subgenual cingulate in schizophrenia. *Eur Arch Psychiatry Clin Neurosci*. Jun 2014;264(4):357-62. doi:10.1007/s00406-013-0482-4
31. Williams MR, Sharma P, Fung KL, Pearce RK, Hirsch SR, Maier M. Axonal myelin increase in the callosal genu in depression but not schizophrenia. *Psychol Med*. Jul 2015;45(10):2145-55. doi:10.1017/S0033291715000136
32. Williams MR, Pattni S, Pearce RK, Hirsch SR, Maier M. Basolateral but not corticomedial amygdala shows neuroarchitectural changes in schizophrenia. *J Neurosci Res*. Jun 2016;94(6):544-7. doi:10.1002/jnr.23683
33. Mignini F, Bronzetti E, Felici L, et al. Dopamine receptor immunohistochemistry in the rat choroid plexus. *J Auton Pharmacol*. Oct-Dec 2000;20(5-6):325-32. doi:10.1046/j.1365-2680.2000.00198.x
34. Townsend JB, Ziedonis DM, Bryan RM, Brennan RW, Page RB. Choroid plexus blood flow: evidence for dopaminergic influence. *Brain Res*. Jan 2 1984;290(1):165-9. doi:10.1016/0006-8993(84)90748-0
35. Castellani G, Contarini G, Mereu M, et al. Dopamine-mediated immunomodulation affects choroid plexus function. *Brain Behav Immun*. Oct 2019;81:138-150. doi:10.1016/j.bbi.2019.06.006
36. Stevens CD, Altshuler LL, Bogerts B, Falkai P. Quantitative study of gliosis in schizophrenia and Huntington's chorea. *Biol Psychiatry*. Oct 1988;24(6):697-700. doi:10.1016/0006-3223(88)90144-8
37. Rothermundt M, Falkai P, Ponath G, et al. Glial cell dysfunction in schizophrenia indicated by increased S100B in the CSF. *Mol Psychiatry*. Oct 2004;9(10):897-9. doi:10.1038/sj.mp.4001548
38. Webster MJ, O'Grady J, Kleinman JE, Weickert CS. Glial fibrillary acidic protein mRNA levels in the cingulate cortex of individuals with depression, bipolar disorder and schizophrenia. *Neuroscience*. 2005;133(2):453-61. doi:10.1016/j.neuroscience.2005.02.037

39. Steiner J, Bernstein HG, Bielau H, et al. S100B-immunopositive glia is elevated in paranoid as compared to residual schizophrenia: a morphometric study. *J Psychiatr Res*. Aug 2008;42(10):868-76. doi:10.1016/j.jpsychires.2007.10.001
40. Williams MR, Hampton T, Pearce RK, et al. Astrocyte decrease in the subgenual cingulate and callosal genu in schizophrenia. *Eur Arch Psychiatry Clin Neurosci*. Feb 2013;263(1):41-52. doi:10.1007/s00406-012-0328-5
41. Bernstein HG, Steiner J, Guest PC, Dobrowolny H, Bogerts B. Glial cells as key players in schizophrenia pathology: recent insights and concepts of therapy. *Schizophr Res*. Jan 2015;161(1):4-18. doi:10.1016/j.schres.2014.03.035
42. Sofroniew MV. Astrocyte barriers to neurotoxic inflammation. *Nat Rev Neurosci*. May 2015;16(5):249-63. doi:10.1038/nrn3898

10.1038/nrn3898.
43. van Kesteren CF, Gremmels H, de Witte LD, et al. Immune involvement in the pathogenesis of schizophrenia: a meta-analysis on postmortem brain studies. *Transl Psychiatry*. 03 2017;7(3):e1075. doi:10.1038/tp.2017.4
44. Kadry H, Noorani B, Cucullo L. A blood-brain barrier overview on structure, function, impairment, and biomarkers of integrity. *Fluids Barriers CNS*. Nov 18 2020;17(1):69. doi:10.1186/s12987-020-00230-3
45. Solár P, Zamani A, Kubíčková L, Dubový P, Joukal M. Choroid plexus and the blood-cerebrospinal fluid barrier in disease. *Fluids Barriers CNS*. May 6 2020;17(1):35. doi:10.1186/s12987-020-00196-2
46. Goldim MPS, Della Giustina A, Petronilho F. Using Evans Blue Dye to Determine Blood-Brain Barrier Integrity in Rodents. *Curr Protoc Immunol*. Sep 2019;126(1):e83. doi:10.1002/cpim.83
47. Liu WY, Wang ZB, Wang Y, et al. Increasing the Permeability of the Blood-brain Barrier in Three Different Models in vivo. *CNS Neurosci Ther*. Jul 2015;21(7):568-74. doi:10.1111/cns.12405
48. del Valle J, Camins A, Pallàs M, Vilaplana J, Pelegrí C. A new method for determining blood-brain barrier integrity based on intracardiac perfusion of an Evans Blue-Hoechst cocktail. *J Neurosci Methods*. Sep 15 2008;174(1):42-9. doi:10.1016/j.jneumeth.2008.06.025
49. Yao L, Xue X, Yu P, Ni Y, Chen F. Evans Blue Dye: A Revisit of Its Applications in Biomedicine. *Contrast Media Mol Imaging*. 2018;2018:7628037. doi:10.1155/2018/7628037
50. Vijayaraghavareddy P, Adhinarayanreddy V, Vemanna RS, Sreeman S, Makarla U. Quantification of Membrane Damage/Cell Death Using Evan's Blue Staining Technique. *Bio Protoc*. Aug 20 2017;7(16):e2519. doi:10.21769/BioProtoc.2519
51. Smith BA, Reider ML, Fletcher JS. Relationship between Vital Staining and Subculture Growth during the Senescence of Plant Tissue Cultures. *Plant Physiol*. Oct 1982;70(4):1228-30. doi:10.1104/pp.70.4.1228
52. Vemanna RS, Babitha KC, Solanki JK, Amarnatha Reddy V, Sarangi SK, Udayakumar M. Aldo-keto reductase-1 (AKR1) protect cellular enzymes from salt stress by detoxifying reactive cytotoxic compounds. *Plant Physiol Biochem*. Apr 2017;113:177-186. doi:10.1016/j.plaphy.2017.02.012
53. Nicoll JAR, Bloom T, Clarke A, Boche D, Hilton D. BRAIN UK: Accessing NHS tissue archives for neuroscience research. *Neuropathol Appl Neurobiol*. Feb 2022;48(2):e12766. doi:10.1111/nan.12766